

# Differential Protein Metabolism and Regeneration in Gastrocnemius Muscles in High-fat Diet Fed Mice and Pre-hibernation Daurian Ground Squirrels: A Comparison between Pathological and Healthy Obesity

Xia Yan<sup>1,2,§</sup>, Qiaohua Niu<sup>2,§</sup>, Xuli Gao<sup>1,2</sup>, Shenyang Shen<sup>2</sup>, Nan He<sup>2</sup>, Huiping Wang<sup>1,2</sup>, Rongrong Fang<sup>2</sup>, Yunfang Gao<sup>1,2,\*</sup>, and Hui Chang<sup>1,2,\*</sup> 

<sup>1</sup>Shaanxi Key Laboratory for Animal Conservation, Northwest University, Xi'an, 710069, P.R. China.

\*Correspondence: E-mail: changhui@nwu.edu.cn (Chang); gaoyunf@nwu.edu.cn (Y. Gao). Tel: +8615389060926. Fax: 029-88303572.  
E-mail: 2364348698@qq.com (Yan); 672622062@qq.com (X. Gao); wanghp@nwu.edu.cn (Wang)

<sup>2</sup>Key Laboratory of Resource Biology and Biotechnology in Western China (College of Life Sciences, Northwest University), Ministry of Education, Xi'an, 710069, P.R. China. E-mail: 1906266475@qq.com (Niu); 2232856399@qq.com (Shen); 1059006214@qq.com (Fang)

<sup>§</sup>XY and QN contributed equally to this work.

Received 27 May 2020 / Accepted 31 December 2020 / Published 8 March 2021  
Communicated by Pung-Pung Hwang

We focused on pathological obesity induced by excessive fat intake (nutritional obesity) in non-hibernator and healthy obesity due to pre-hibernation (PRE) fat storage in hibernator to study the effects of different types of obesity on skeletal muscle protein metabolism and cell regeneration. Kunming mice were fed with high-fat diet for 3 months to construct a pathological obesity model. Daurian ground squirrels fattened naturally before hibernation were used as a healthy obesity model. Body weight, adipose tissue wet weight, gastrocnemius muscle wet weight, muscle fiber cross-sectional area (CSA) and fiber type distribution were measured. The protein expression levels related to protein degradation (MuRF-1, atrogin-1, calpain1, calpain2, calpastatin, desmin, troponin T, Beclin-1, LC3-II), protein synthesis (P-Akt, P-mTORC1, P-S6K1, P-4E-BP1) and cell regeneration (MyoD, myogenin, myostatin) were detected by Western blot. As a result, the body weight and adipose tissue wet weight were both significantly increased in high fat obese (OB) mice and pre-hibernation fat (PRE) ground squirrels. The muscle wet weight, ratio of muscle wet weight to body weight, and muscle fiber CSA were significantly decreased, while the percentage of MHC I fiber isoform was significantly increased in gastrocnemius muscle of OB mice compared with the control (CON) group. The protein expression levels of P-Akt, P-mTORC1, P-4E-BP1 and myogenin were significantly decreased, while those of calpain1, calpain2, MuRF-1 and myostatin were significantly increased in the OB mice. In the ground squirrels, the muscle wet weight, muscle fiber CSA and percentage of MHC I fiber isoform all showed no change in the gastrocnemius muscle in the PRE group compared with the summer active (SA) group. The protein expression levels of P-Akt, P-mTORC1, P-S6K1 and MyoD were significantly increased, while those of Beclin-1 and LC3-II were significantly decreased in the PRE ground squirrels. This study demonstrated that the decrease in protein expression levels in the Akt/mTOR pathway (P-Akt, P-mTORC1 and P-4E-BP1) and cell regeneration (myogenin) and the increase in protein expression levels of the calpain pathway (calpain1 and calpain2) and ubiquitin-proteasome pathway (MuRF-1) were involved in the mechanism of muscle atrophy in gastrocnemius muscle of the pathologically obese Kunming mice induced by high-fat diet. In contrast, the increased protein expression

Citation: Yan X, Niu Q, Gao X, Shen S, He N, Wang H, Fang R, Gao Y, Chang H. 2021. Differential protein metabolism and regeneration in gastrocnemius muscles in high-fat diet fed mice and pre-hibernation Daurian ground squirrels: a comparison between pathological and healthy obesity. Zool Stud 60:6. doi:10.6620/ZS.2021.60-06.

levels of the Akt/mTOR pathway (P-Akt, P-mTORC1 and P-S6K1) and cell regeneration (MyoD), and the decreased protein expression levels of the autophagy lysosomal pathway (Beclin-1 and LC3-II) were involved in the mechanism of anti-atrophy in gastrocnemius muscle of the healthy obese ground squirrels fattened before hibernation.

**Key words:** High-fat diet, Pre-hibernation fattening, Protein metabolism, Cell regeneration, Skeletal muscle atrophy.

## BACKGROUND

Skeletal muscle accounts for more than 40% of a mammal's weight, and is not only the main organ for providing physical strength and exercise but also the main place for material and energy consumption (Chang et al. 2016; Li and Ji 2018). Nutritional obesity causes skeletal muscle atrophy; it occurs in a variety of muscles, including the gastrocnemius muscle, soleus muscle and tibialis anterior muscle (Adhikary et al. 2019; Akhmedov and Berdeaux 2013; Lee et al. 2018; Tong et al. 2019), and is mainly characterized by a decrease in muscle mass, reduction in cross-sectional area of muscle fibers, and changes in the types of fiber and myosin isoforms (Dumitru et al. 2018; Tong et al. 2019). Meanwhile, the expressions of atrogen-1 and MuRF-1, as atrogenes, are up-regulated in muscle atrophy induced by obesity (Adhikary et al. 2019; Bodine and Baehr 2014).

Interestingly, lipid-storing hibernating species acquire and store large amounts of fat during the pre-hibernation fattening stage, and then go into hibernation. After the fat storage and before hibernation, the weight of the hibernator is often increased greatly (Xing et al. 2012). However, at least in hibernators like Japanese black bears (*Ursus thibetanus japonicus*), the obesity in pre-hibernation is not accompanied by a series of health problems, such as type 2 diabetes and hyperglycemia, which are common in non-hibernators with the same percentage of fat (Kamine et al. 2012). Thus, the obesity in hibernators caused by the fattening before hibernation is called "healthy obesity" (Rigano et al. 2017). Our previous research showed that there was no change in the muscle wet weight and cross-sectional area in gastrocnemius muscle, plantaris muscle or extensor digitorum longus muscle between the pre-hibernation (PRE, squirrels that finished natural fattening in late-autumn) and the summer active (SA, squirrels that were in active state in June) Daurian ground squirrels (*Spermophilus dauricus*) (Zhang et al. 2019; Ma et al. 2019). Therefore, the gastrocnemius muscle, the largest muscle on the calf of the ground squirrel, does not undergo muscle atrophy during fat storage and before

hibernation.

Skeletal muscle atrophy is caused by an imbalance in protein synthesis and degradation (Schiaffino et al. 2013). Protein synthesis is mainly regulated by the insulin-like growth factor-1 (IGF-1)/protein kinase B (PKB, also called Akt) signaling pathway, which affects the transcription and translation processes in protein synthesis by activating the mammalian target of rapamycin (mTOR) (Andres-Mateos et al. 2013). In this pathway, ribosomal protein S6 kinase 1 (S6K1) and eukaryotic initiation factor 4E binding protein 1 (4E-BP1) are the most critical downstream effectors of mammalian target of rapamycin in complex 1 (mTORC1) (Gao et al. 2018). The reduced activations of Akt, p70S6K and mTOR result in reduced protein synthesis and reduced muscle growth in the plantaris muscle of male obese C57BL/6 mice (*Mus musculus*) induced by a 14-week high-fat and low-carbohydrate diet, the gastrocnemius muscle of male obese Wistar rats (*Rattus norvegicus*) induced by a 16-week high-fat and high-carbohydrate Western-type diet, and the gastrocnemius muscle of male obese C57BL/6 mice induced by a 10-week high-fat diet (Sishi et al. 2011; Sitnick et al. 2009; Tong et al. 2019). However, it has been reported that there is no difference in P-mTOR or P-Akt levels in the muscles of grizzly bears (*Ursus arctos horribilis*) after finishing fattening before hibernation (in October) compared with the SA period (in May) (Rigano et al. 2017). In view of the differential expression of proteins and the possible changes in skeletal muscle, it is necessary to further compare the expression of the Akt-mTOR signal in the two rodent obesity models.

Protein degradation in skeletal muscle involves the calpain pathway, the ubiquitin-proteasome pathway, the autophagy lysosomal pathway and others (Jackman and Kandarian 2004). Calpain is the initiator of skeletal muscle protein degradation, which triggers the activation of the ubiquitin-proteasome pathway (Jackman and Kandarian 2004). Calpain1 can be activated by micromolar  $Ca^{2+}$ , and calpain2 requires millimolar  $Ca^{2+}$  to be activated; these are the two most widely studied isozyme molecules (Goll et al. 2003).

Calpastatin is a specific, endogenous inhibitor of calpain (Goll et al. 2003). It has been reported that there are higher calpain1 and calpain2 mRNA levels in skeletal muscles in 5-month-old male obese (fa/fa) Zucker rats than in lean rats when they are in a sedentary state (Hsieh et al. 2008). However, our previous study reported that the protein expression levels of calpain1, calpain2 and calpastatin show no difference between the PRE and SA group in the lateral gastrocnemius muscle, plantaris muscle and extensor digitorum longus muscle in Daurian ground squirrels (Ma et al. 2019). The ubiquitin-proteasome pathway includes three catalytic proteins: ubiquitin-activating enzyme E1, ubiquitin-binding enzyme E2s and ubiquitin-protein ligase E3s (Hershko and Ciechanover 1998). Atrogin-1 and muscle ring finger-1 (MuRF-1) are two of the most common E3s (Glass 2005). MuRF-1 level was significantly increased by 97.4%, while atrogin-1 showed no change in the gastrocnemius muscle of male obese Wistar rats induced by 16 weeks of high-fat and high-carbohydrate Western-type diet feeding (Sishi et al. 2011). However, in Daurian ground squirrels, the expression levels of MuRF-1 and atrogin-1 in the lateral gastrocnemius muscle, plantaris muscle, extensor digitorum longus muscle were not changed between the pre-hibernation group and the SA group (Ma et al. 2019). The other pathway involved in protein degradation is the autophagy lysosomal pathway (Sandri 2008). Autophagy is a highly conserved pathway responsible for the hydrolysis of long-lived proteins and organelles in cells (Sala et al. 2014), which maintains homeostasis by degrading the cell's own components and is usually activated in conditions of nutrient deprivation or starvation (Mizushima et al. 2004; Mordier et al. 2000). Beclin-1 is one of the important components of the Class III Phosphatidylinositol-3-kinase (PI3KC3) complex and plays a necessary role in the process of autophagosome nucleation (Mei et al. 2016). Microtubule-associated protein 1A/1B-light chain 3 (LC3) is another important molecule near the downstream of the autophagic pathway and is involved in the formation of autophagosomes, which is an indicator of autophagy lysosomal pathway activation (Klionsky et al. 2012). Previous studies showed that the expression of LC3 did not change between the obesity and control groups in the gastrocnemius muscle of C57BL/6 male mice induced by a 10-week high-fat diet (Herrenbruck and Bollinger 2019). Similarly, the expression of LC3, LC3-II/I and Beclin-1 was also not significantly different between the obesity and control group in the soleus muscle and plantaris muscle of female Sprague Dawley rats induced by a 16-week high-fat diet (Campbell et al. 2015). However, the protein expression level of Beclin-1 in the soleus

muscle was significantly increased, while the protein expression levels of LC3-II and the ratio of LC3-II/I were significantly decreased in pre-hibernation group compared with SA group in Daurian ground squirrels (Chang et al. 2020). Excessive protein degradation causes muscle mass loss and promotes muscle atrophy. Therefore, our study selected the largest skeletal muscle of the hind calf—the gastrocnemius muscle to study the role of the calpain pathway, the ubiquitin-proteasome pathway and the autophagy lysosomal pathway in muscle atrophy in the pathological obesity model and the healthy obesity model.

Maintenance of skeletal muscle mass is also associated with cell regeneration (Sartorelli and Fulco 2004). During the regeneration of skeletal muscle cells, the expression of myogenicity differentiation factor (MyoD) and myogenin play an important role in the proliferation and differentiation of satellite cells (Akhmedov and Berdeaux 2013). However, myostatin, a negative regulator of cell regeneration, can reduce myocyte proliferation and differentiation (Lee 2004) and inhibit the expression of MyoD and myogenin (Akhmedov and Berdeaux 2013). It has been reported that the obese mice induced by a high-fat diet display attenuated muscle regeneration after injury more than control mice (D'Souza et al. 2015). In addition, the expression of myostatin in skeletal muscle was increased in high-fat diet and ob/ob mice as well as in extremely obese women (Allen et al. 2008; Hittel et al. 2009). Therefore, it is necessary to clarify whether the regeneration is different in skeletal muscle between the pathological obesity model and the healthy obesity model.

Why do pre-hibernation ground squirrels prevent skeletal muscle atrophy caused by fattening before hibernation? Based on the previous research on protein metabolism, we hypothesize that the skeletal muscle can be maintained through regulating protein synthesis, degradation and cell regeneration in the healthy obesity ground squirrels caused by pre-hibernation fattening, which is different from the muscle atrophy in pathologically obese mice induced by high-fat diet. In this study, the Daurian ground squirrels after natural fattening were used as a healthy animal model of obesity, whereas the Kunming mice fed with high-fat diet for 3 months were used as a pathological model of nutritional obesity. We examined the body weight, the adipose tissue wet weight, the muscle wet weight, the cross-sectional area, the muscle fiber type and the protein expressions of MuRF-1, atrogin-1, calpain1, calpain2, calpastatin, troponin T, desmin, Beclin-1, LC3-II, P-Akt, P-mTORC1, P-S6K1, P-4E-BP1, MyoD, myogenin and myostatin, intending to compare and clarify the similarities and differences

of protein expression levels of key signal molecules related to protein metabolism and cell regeneration in gastrocnemius muscle between pathological obesity and healthy obesity, which will provide experimental evidence for screening key targets for anti-atrophy induced by obesity in fattening before hibernation.

## MATERIALS AND METHODS

### Animal model of pathological obesity

All animal experiments were approved by the Experimental Animal Protection Committee of the Ministry of Health of the People’s Republic of China. Four-week-old male Kunming mice, weighing 23 to 25 grams, were purchased from Chengdu Dashuo Experimental Animal Company. The mice were placed in plastic cages with sawdust. There were 2–3 mice per cage, and food and water were provided *ad libitum*. They were kept in a standard animal room at 18–25°C where the light and darkness corresponded to the local sunrise and sunset. The sawdust in the cage was replaced every two days to keep it clean. The mice were randomly divided into two groups after being fed a normal diet for one week. (1) Control group (CON group,  $n = 6$ ): fed with normal diet; (2) obesity group (OB group,  $n = 6$ ): fed with high-fat diet, as the pathological obesity model. The normal feed and high-fat feed were provided by Chengdu Dashuo Experimental Animal Company. Individuals were then stored at room temperature and protected from light. The composition of normal diet and high fat diet is shown in table 1. After feeding for 3 months, both groups of mice were sacrificed and sampled.

### Animal model of healthy obesity

As described by our laboratory previously

(Chang et al. 2018), the Daurian ground squirrels were captured from the Weinan plain in the Shaanxi province of China. After returning to the laboratory, all ground squirrels were put in plastic cages with sawdust, with one ground squirrel per cage; food and water were provided *ad libitum*. The ground squirrels were maintained in an animal room at 18–25°C where the light and darkness corresponded to the local sunrise and sunset. The sawdust in the cage was replaced every two days to keep it clean. There were two groups of ground squirrels in the experiment ( $n = 6$ , three females and three males in each group): (1) Summer active group (SA group): active squirrels in June with a body temperature (Tb) of 36–38°C; captured and sacrificed in end of June. (2) Pre-hibernation group (PRE group): squirrels that had finished fattening in nature; captured and sacrificed in late-autumn (end of September, 30–40 d before hibernation).

### Sample collection

After the body weight was recorded, the mice were anesthetized with 2 mg/kg sodium pentobarbital intraperitoneally, while the ground squirrels were anesthetized with 90 mg/kg sodium pentobarbital intraperitoneally. Then the gastrocnemius muscles from both legs were separated and weighed immediately. Subsequently, the muscle samples were frozen in liquid nitrogen and stored at -80°C for follow-up experiments. The adipose tissues—including mesenteric adipose, perirenal adipose and back scapula subcutaneous adipose—were also separated and weighed. The animals were sacrificed by an overdose injection of sodium pentobarbital after sampling was completed.

### Immunofluorescent analysis

The muscle fiber cross-sectional area (CSA) and fiber type composition were measured by

**Table 1.** Composition of the experimental diets

(A) Composition of normal diet		(B) Composition of high fat diet	
Components	Content	Components	Content
Corn	25.4 g	Patterned animal base	50 g
Wheat	30.6 g	Soy flour	5 g
Soybean	13 g	Fish meal	5 g
Fish meal	6 g	Milk powder	10 g
Rice bran	6 g	Peanut	6 g
Wheat bran	10 g	Egg yolk powder	5 g
Soybean meal	5 g	Lard	12 g
Other	4 g	Salt	2 g
Total	100g	Sucrose	5 g

immunofluorescent analysis, as described by our laboratory previously (Chang et al. 2018). Briefly, the mid-belly of gastrocnemius muscle was cut into 10- $\mu$ m thick frozen muscle cross-sections at  $-20^{\circ}\text{C}$  with a cryostat (Leica, Wetzlar, CM1850, Germany). Then the slides with sections were fixed in 4% paraformaldehyde for 30 min, and subsequently permeabilized in 0.1% Triton X-100 (dissolve in PBS) for 30 min. The slides were then blocked with 1% bovine serum albumin (BSA) in PBS for 60 min at room temperature, and immediately incubated at  $4^{\circ}\text{C}$  overnight with the anti-laminin rabbit polyclonal antibody (1:200, Boster, BA1761-1) to visualize the myofiber interstitial tissue and the anti-skeletal slow myosin mouse monoclonal antibody (1:200, Boster, BM1533) to visualize the type I MHC in both muscles. The slides were rinsed twice in PBS and incubated with Alexa Fluor 647-labeled IgG secondary antibody (1:200; Thermo Fisher Scientific, #A21245) and FITC-labeled IgG secondary antibody (1:200; Sigma, F1010) for 60 min. Image-Pro Plus 6.0 software was used to measure the CSA of at least 10 different visual fields of each sample.

### Western blots

As described previously by our lab (Chang et al. 2018). The total protein, extracted from the frozen gastrocnemius muscles of mice and ground squirrels by homogenization, was put into a sample buffer (pH 6.8, 100 mM Tris, 4% SDS, 5% glycerol, 5% 2- $\beta$ -mercaptoethanol, and bromophenol blue). Then, the muscle protein extracts were separated by SDS-PAGE (10% Laemmli gels with an acrylamide/bisacrylamide ratio of 29:1 for P-Akt, P-mTORC1, P-S6K1, P-4E-BP1, calpain1, calpain2, calpastatin, troponin T, desmin, atrogen-1, MuRF-1, Beclin-1, LC3, MyoD, myogenin and myostatin). After electrophoresis, the total protein bands were visualized by putting the gel on the UV transilluminator and irradiating for 2 min; the Syngene G:BOX system (Syngene, Frederick, MD) was then used to take photographs of the gel. The protein gel was transferred electrically to PVDF membranes (0.45  $\mu$ m) using a Bio-Rad semi-dry transfer apparatus. Then, the membranes were blocked with 5% skim milk dissolved in TBST (10 mM Tris-HCl, 150 mM NaCl, 0.05% Tween-20, pH 7.6) for 2 h at room temperature and incubated with the primary antibodies of P-Akt (Ser473) (1:1,000, abcam, 81283), P-mTORC1 (Ser2448) (1:1,000, sigma, 4504476), P-S6K1 (Thr389) (1:1,000, Cell Signaling Technology (CST), 9205S), P-4E-BP1 (Thr37/46) (1:1,000, CST, 2855S), calpain1 (1:1,000, CST, 2556S), calpain2 (1:1,000, CST, 2539S), calpastatin (1:1,000, CST, 4146S), troponin T (1:1,000, Sigma, T6277), desmin (1:1,000, CST, 4024S), atrogen-1

(1:1,000, Proteintech, 12866-1-AP), MuRF-1 (1:1000, Abcam, ab172479), Beclin-1 (1:1000, CST, 3738), LC3 (1:1000, abcam, ab48394), MyoD (1:1,000, proteintech, 18943-1-AP), myogenin (1:1,000, abcam, 124800) and myostatin (1:1,000, proteintech, 19142-1-AP) in TBST containing 0.1% bovine serum albumin (BSA) at  $4^{\circ}\text{C}$  overnight. Then the membrane was washed with TBST four times (10 minutes/time) and incubated with HRP-conjugated anti-mouse secondary antibody (1:10000, Thermo Fisher Scientific, A28177) or HRP-conjugated anti-rabbit secondary antibody (1:5000, Thermo Fisher Scientific, A27036) for 2 h at room temperature. Then the PVDF membrane was washed three times (10 min/time). The fluorescent bands were visualized using enhanced chemiluminescence reagents (Thermo Fisher Scientific, NCI5079). The NIH Image J software was used to carry out quantification analysis. The density of the immunoblot band in each individual lane was standardized using the summed densities from a group of total protein bands in the same lane.

### Statistical analyses

An independent-samples *t*-test was used to determine the significant differences between OB and CON mice, SA and PRE ground squirrels. All western blot data were corrected for false discovery rate (FDR). All data were analyzed using SPSS 24 and expressed as means  $\pm$  SEM.  $p < 0.05$  was considered to be statistically significant.

## RESULTS

### Body weight

The composition of normal diet and high fat diet is shown in table 1. The fat calorie percentage of high fat diet is 61%. As shown in table 2, after being fed a high-fat diet or normal diet for 3 months, the OB mice gained 10.6% higher body weight than the CON group (CON:  $46.3 \pm 0.5$  g vs. OB:  $51.2 \pm 1.1$  g,  $p < 0.05$ ). In ground squirrels, the body weight of the PRE group was significantly increased by 67.9% (SA:  $200.3 \pm 2.0$  g vs. PRE:  $336.3 \pm 15.6$  g,  $p < 0.05$ ) compared with the SA group at experiment time.

### Adipose tissue wet weight, muscle wet weight and the ratio of muscle wet weight to body weight

As shown in table 3, compared with the CON mice, the mesenteric adipose wet weight in the OB group was significantly increased by 1.1-fold from

0.89 g to 1.89 g ( $p < 0.05$ ), while the perirenal adipose wet weight was significantly increased by 1.1-fold from 0.30 g to 0.63 g ( $p < 0.05$ ). Compared with the SA ground squirrels, the mesenteric adipose wet weight in the PRE group was significantly increased by 24.4-fold from 0.74 g to 18.78 g ( $p < 0.05$ ), the perirenal adipose wet weight was significantly increased by 8.8-fold from 0.32 g to 3.13 g ( $p < 0.05$ ), and the subcutaneous adipose wet weight was significantly increased by 34.6-fold from 0.35 g to 12.47 g ( $p < 0.05$ ).

As shown in figure 1A, the wet weight of the gastrocnemius muscle in the OB mice was significantly reduced by 8.8% from 361.75 mg to 329.80 mg

compared with the CON group ( $p < 0.05$ ). However, there was no change in the gastrocnemius muscle wet weight between the PRE and SA ground squirrels.

As shown in figure 1B, the ratio of muscle wet weight/body weight was significantly decreased by 17.4% in the OB mice compared with the CON group ( $p < 0.05$ ), while the ratio was significantly decreased by 40.3% in the PRE ground squirrels compared with the SA group ( $p < 0.05$ ).

### Fiber type distribution and fiber CSA

The fiber type distribution and CSA of the

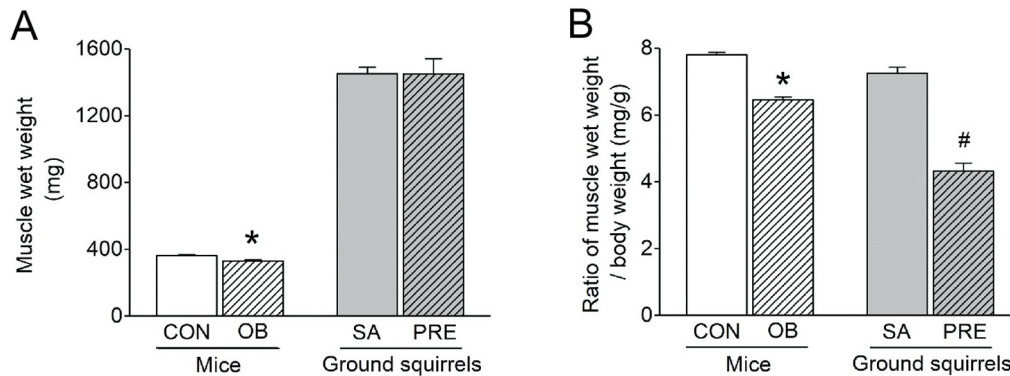


**Fig. 1.** Skeletal muscle wet weight and the ratio of muscle wet weight/body weight. (A) The changes in muscle wet weight in mice and Daurian ground squirrels. (B) The changes in the ratio of muscle wet weight/body weight in mice and Daurian ground squirrels. CON: control mice, OB: mice after 3 months of ingesting high fat diet, SA: summer active Daurian ground squirrels, PRE: pre-hibernation, squirrels that finished natural fattening, sacrificed in late-autumn (end of September, 30–40 d before hibernation). Values are mean  $\pm$  SEM,  $n = 6$ . \* $p < 0.05$  compared with CON group. # $p < 0.05$  compared with SA group.

**Table 2.** Body weight for all groups

	CON	OB	SA	PRE
Body weight before high fat-fed (g)	24.1 $\pm$ 0.3	24.5 $\pm$ 0.2	-	-
Body weight at experiment time (g)	46.3 $\pm$ 0.5	51.2 $\pm$ 1.1 *	200.3 $\pm$ 2.0	336.3 $\pm$ 15.6 #

CON: control mice, OB: mice after 3 months of ingesting high fat diet, SA: summer active Daurian ground squirrels, PRE: pre-hibernation, squirrels that finished natural fattening, sacrificed in late-autumn (end of September, 30–40 d before hibernation). Values are mean  $\pm$  SEM,  $n = 6$ . \* $p < 0.05$  compared with CON group. # $p < 0.05$  compared with SA group.

**Table 3.** Adipose tissue wet weight

	CON	OB	SA	PRE
Mesenteric adipose wet weight (g)	0.89 $\pm$ 0.12	1.89 $\pm$ 0.21 *	0.74 $\pm$ 0.20	18.78 $\pm$ 2.74 #
Perirenal adipose wet weight (g)	0.30 $\pm$ 0.03	0.63 $\pm$ 0.08 *	0.32 $\pm$ 0.13	3.13 $\pm$ 0.37 #
Subcutaneous adipose wet weight (g)	-	-	0.35 $\pm$ 0.17	12.47 $\pm$ 1.15 #

CON: control mice, OB: mice after 3 months of ingesting high fat diet, SA: summer active Daurian ground squirrels, PRE: pre-hibernation, squirrels that finished natural fattening, sacrificed in late-autumn (end of September, 30–40 d before hibernation). Values are mean  $\pm$  SEM,  $n = 6$ . \* $p < 0.05$  compared with CON group. # $p < 0.05$  compared with SA group.

gastrocnemius muscle fibers were measured by immunofluorescent staining. As shown in figure 2B, the percentage of MHC I fiber isoform in the gastrocnemius muscles was significantly increased (58.1%,  $p < 0.05$ ) in the OB mice compared with the CON group, whereas it had no significant difference between the PRE and SA ground squirrels.

Compared with the CON mice, the CSA of the gastrocnemius muscle was significantly reduced (-14.7%,  $p < 0.05$ ) in the OB group, whereas it was not significantly different between the PRE and SA ground squirrels (Fig. 2C).

### Relative protein levels of MuRF-1 and atrogen-1

We analyzed the expression levels of MuRF-1 and atrogen-1, which are molecular markers of muscle atrophy and the E3s in the ubiquitin proteasome pathway (Bodine et al. 2001). Compared with the CON mice, the expression of MuRF-1 was significantly increased in the OB group (18.1%,  $p < 0.05$ ), while it was not significantly different between the PRE and SA ground squirrels (Fig. 3B). The expression level of

atrogen-1 showed no change in the CON or OB mice. In addition, there was no significant difference in the PRE or SA ground squirrels (Fig. 3C).

### Relative protein levels of calpain1, calpain2, calpastatin, desmin and troponin T

We determined the molecules in the calpain pathway that initiate protein degradation, including calpain1 and calpain2, which act on degradation, their inhibitor calpastatin, and their substrates desmin and troponin T (Yang et al. 2014). The expression levels of calpain1 and calpain2 were significantly increased in the gastrocnemius muscle in the OB mice (60.1% and 22.4%, respectively,  $p < 0.05$ ) compared with the CON group, while there was no significant difference between the PRE and SA ground squirrels (Fig. 4B and 4C). The expression level of calpastatin showed no significant difference between the OB and CON mice, or between the PRE and SA ground squirrels (Fig. 4D). As the substrates of calpain, both desmin and troponin T showed a significant decrease in the OB mice compared with the CON group (-33.6% and -29.8%, respectively,

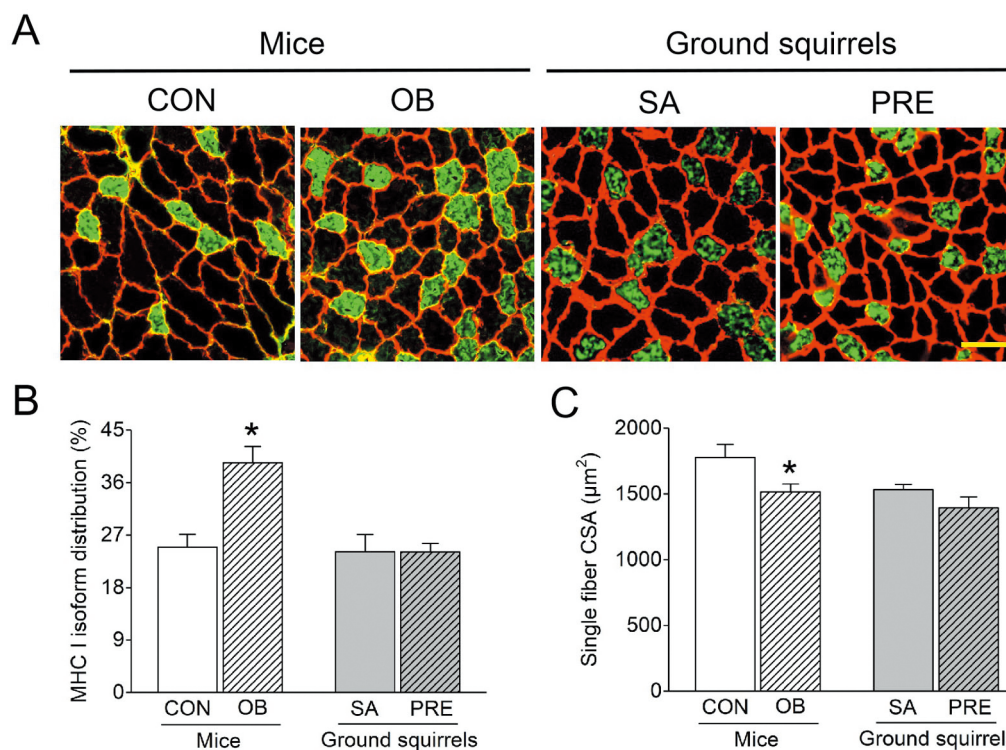


**Fig. 2.** MHC I isoform distribution and single fiber cross-sectional area (CSA). (A) Representative immunofluorescent images of MHC I (green) fibers in gastrocnemius muscles in each group. Red represents laminin stain of myofiber interstitial tissue. Scale bar = 50  $\mu\text{m}$ . (B) The changes in MHC I isoform distribution (%) in mice and Daurian ground squirrels. (C) The changes in muscle single fiber CSA in mice and Daurian ground squirrels. CON: control mice, OB: mice after 3 months of ingesting high fat diet, SA: summer active Daurian ground squirrels, PRE: pre-hibernation, squirrels that finished natural fattening, sacrificed in late-autumn (end of September, 30–40 d before hibernation). Values are mean  $\pm$  SEM,  $n = 6$ . \* $p < 0.05$  compared with CON group.

$p < 0.05$ ). However, both desmin and troponin T was not significantly different between the PRE and SA ground squirrels (Fig. 4E and 4F).

**Relative protein levels of Beclin-1 and LC3-II**

Beclin-1 and LC3-II are important molecules in the autophagy pathway of protein degradation (Chang et al. 2020). Compared with the CON mice, the expression levels of Beclin-1 and LC3-II had no significant differences in the OB group. However, both Beclin-1 and LC3-II were significantly decreased in the PRE ground squirrels compared with the SA group (-11.8% and -35.5%, respectively,  $p < 0.05$ , Fig. 5B and 5C).

**Relative protein levels of P-Akt, P-mTORC1, P-S6K1 and P-4E-BP1**

The Akt//mTOR pathway is an important way to regulate protein synthesis, and S6K1 and 4E-BP1 are the most important effectors downstream of mTORC1 (Schiaffino et al. 2013). Here, we measured

the expression levels of phosphorylated Akt, mTORC1, S6K1 and 4E-BP1 to compare the differences in protein synthesis in obesity mice and ground squirrels. As shown in figure 6, the relative protein levels of P-Akt and P-mTORC1 were significantly decreased in the OB mice compared with the CON group (-33.8% and -25.0%, respectively,  $p < 0.05$ ). In contrast, both P-Akt and P-mTORC1 were significantly increased in the PRE ground squirrels compared with the SA group (22.3% and 28.9%, respectively,  $p < 0.05$ , Fig. 6B and 6C). The relative protein level of P-S6K1 showed no change between the OB and CON group in mice (Fig. 6D), while it was significantly increased in the PRE ground squirrels compared with that in the SA group (30.5%,  $p < 0.05$ , Fig. 6D). In addition, the protein expression level of P-4E-BP1 in the OB mice was significantly decreased compared with the CON group (-26.1%,  $p < 0.05$ ), while it showed an increased trend but no significant difference in the PRE ground squirrels compared with that in the SA group (40.1%,  $p = 0.05$ , Fig. 6E).

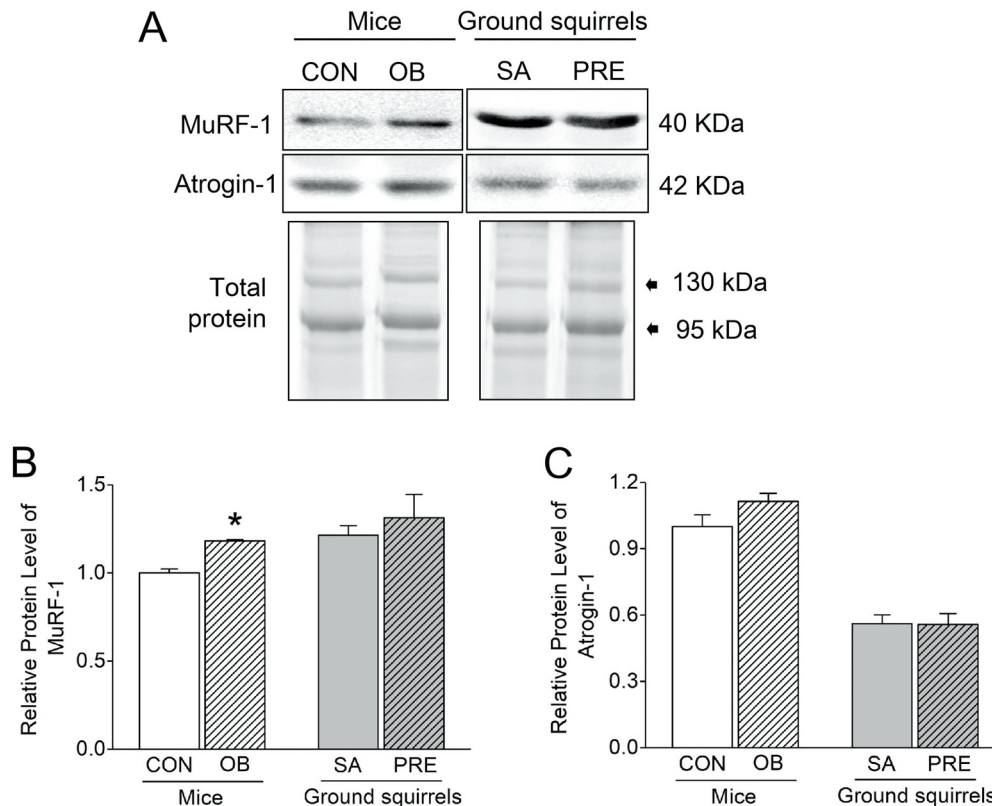


**Fig. 3.** The protein expression levels of MuRF-1 and atrogin-1. (A) Representative immunoblots of MuRF-1 and atrogin-1 in gastrocnemius muscles in each group. (B) The relative protein expression level of MuRF-1 in mice and Daurian ground squirrels. (C) The relative protein expression level of atrogin-1 in mice and Daurian ground squirrels. CON: control mice, OB: mice after 3 months of ingesting high fat diet, SA: summer active Daurian ground squirrels, PRE: pre-hibernation, squirrels that finished natural fattening, sacrificed in late-autumn (end of September, 30–40 d before hibernation). Values are mean ± SEM,  $n = 6$ . \* $p < 0.05$  compared with CON group.



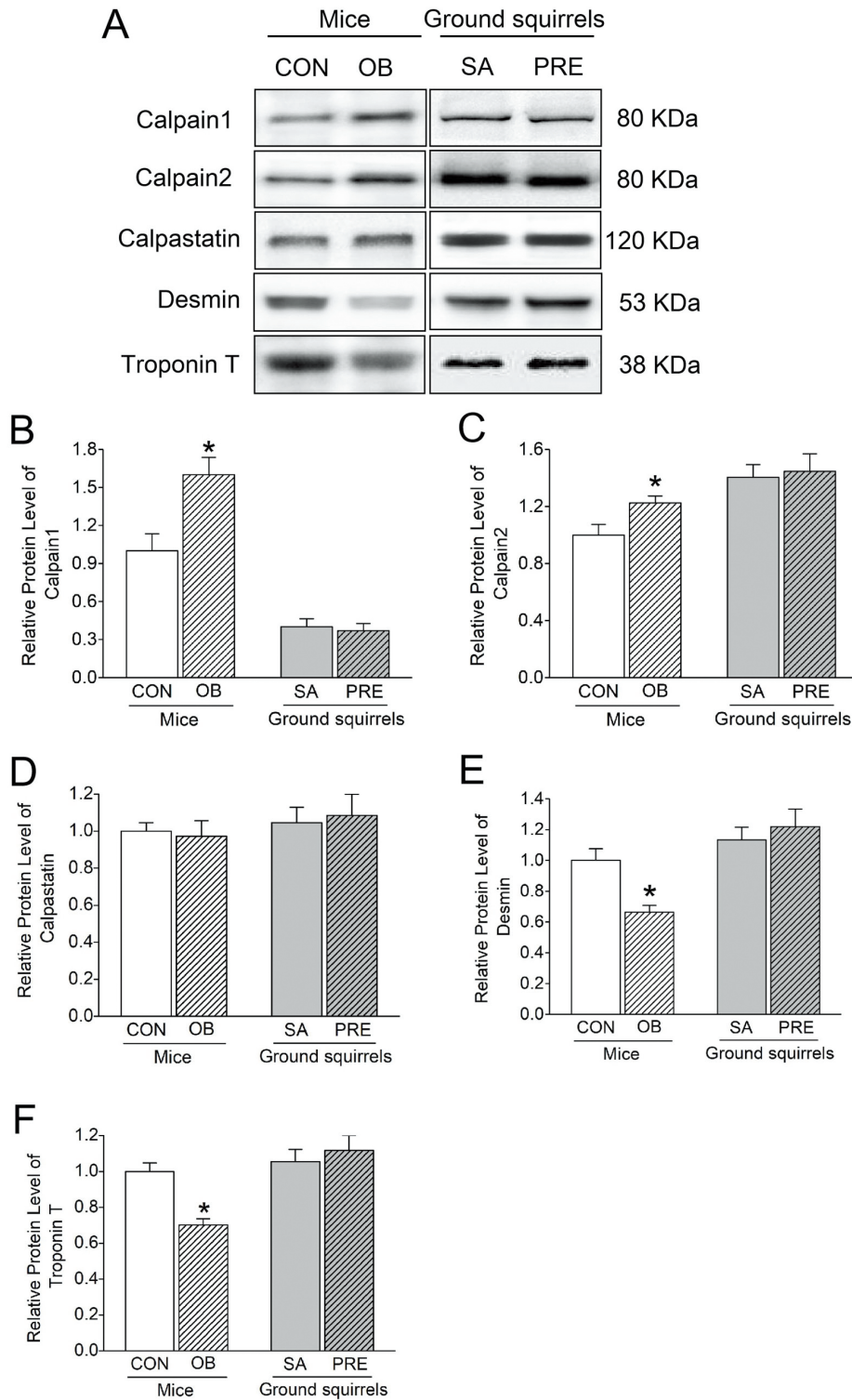


**Fig. 4.** The protein expression levels of calpain1, calpain2, calpastatin, desmin and troponin T. (A) Representative immunoblots of calpain1, calpain2, calpastatin, desmin and troponin T in gastrocnemius muscles in each group. (B) The relative protein expression level of calpain1 in mice and Daurian ground squirrels. (C) The relative protein expression level of calpain2 in mice and Daurian ground squirrels. (D) The relative protein expression level of calpastatin in mice and Daurian ground squirrels. (E) The relative protein expression level of desmin in mice and Daurian ground squirrels. (F) The relative protein expression level of troponin T in mice and Daurian ground squirrels. CON: control mice, OB: mice after 3 months of ingesting high fat diet, SA: summer active Daurian ground squirrels, PRE: pre-hibernation, squirrels that finished natural fattening, sacrificed in late-autumn (end of September, 30-40 d before hibernation). Values are mean  $\pm$  SEM,  $n = 6$ . \* $p < 0.05$  compared with CON group.

### Relative protein levels of MyoD, myogenin and myostatin

We also determined the molecular expression of regeneration pathway related to maintaining muscle mass, including MyoD and myogenin, which promotes the proliferation and differentiation of satellite cells (Chen and Shan 2019), and myostatin, a negative regulator of muscle growth (Ohno et al. 2016). As shown in figure 7, the relative protein level of MyoD showed no significant difference between the OB and CON mice, while it was significantly increased in the PRE ground squirrels compared with the SA group (39.2%,  $p < 0.05$ , Fig. 7B). The expression level of myogenin was significantly decreased in the OB mice compared with the CON group (-31.0%,  $p < 0.05$ ), while it showed an increased trend but no significant difference in the PRE ground squirrels compared with the SA group (21.6%,  $p = 0.08$ , Fig. 7C). Moreover, the expression of myostatin in the OB mice was significantly increased by 42.7% compared with that in the CON group ( $p < 0.05$ ), but showed no change between the PRE and SA ground squirrels (Fig. 7D).

### DISCUSSION

In this study, we innovatively compared the differences in protein metabolism and regeneration

related protein expression levels in gastrocnemius muscle between the pathological obesity model induced by high-fat diet (mice) and the healthy obesity model fattened before hibernation (ground squirrels). We detected body weight, adipose tissue wet weight, gastrocnemius muscle wet weight, cross-sectional area, fiber type distribution, and the relative expression levels of proteins which related to protein synthesis, degradation and cell regeneration. Our results showed that the gastrocnemius muscle exhibited opposite effects of muscle atrophy and anti-atrophy in pathologically obese mice and healthy obese ground squirrels, which was caused by the differential regulation of protein synthesis, degradation and cell regeneration (Fig. 8 and Table 4). Although some controversial views may focus on the differences in body size and living environment between mice and ground squirrels, they are all rodents at least, and the atrophy and anti-atrophy in gastrocnemius muscle are affirmatory in the two species, respectively. Perhaps other hibernating animals can be used as a potential research model for anti-obesity muscular atrophy.

Both the OB mice and the PRE ground squirrels showed a significant increase in body weight (Table 2) and adipose tissue wet weight (Table 3). The body weight of the OB mice increased by nearly 10.6% compared with the CON group, while the body weight showed a higher increase by 67.9% in the PRE ground squirrels compared with the SA group (Table 2). In

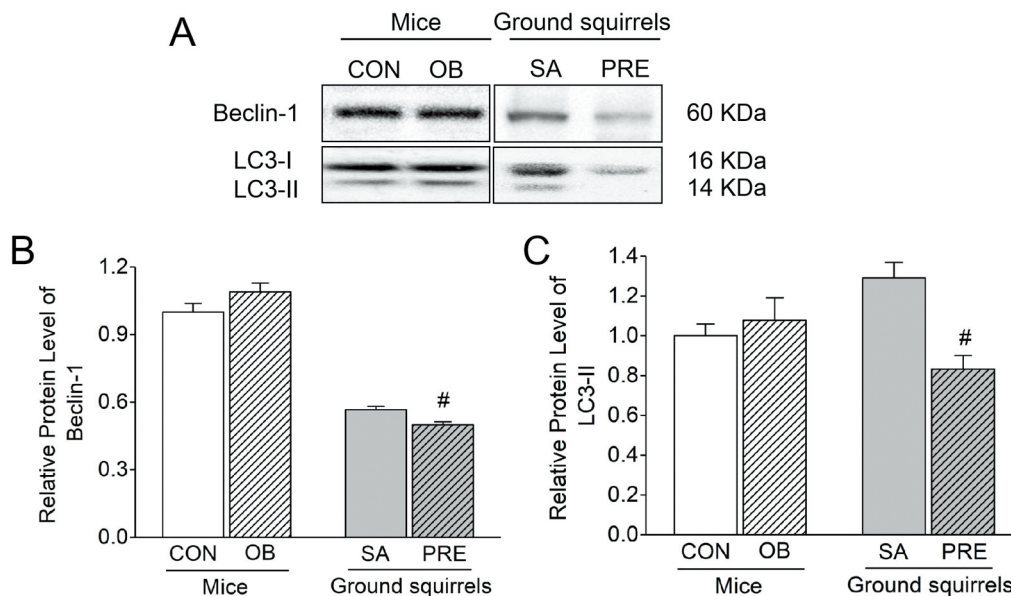


**Fig. 5.** The protein expression levels of Beclin-1 and LC3-II. (A) Representative immunoblots of Beclin-1 and LC3 in gastrocnemius muscles in each group. (B) The relative protein expression level of Beclin-1 in mice and Daurian ground squirrels. (C) The relative protein expression level of LC3-II in mice and Daurian ground squirrels. CON: control mice, OB: mice after 3 months of ingesting high fat diet, SA: summer active Daurian ground squirrels, PRE: pre-hibernation, squirrels that finished natural fattening, sacrificed in late-autumn (end of September, 30–40 d before hibernation). Values are mean  $\pm$  SEM,  $n = 6$ . # $p < 0.05$  compared with SA group.

addition, our data showed that the increase in adipose tissue wet weight in the OB mice was mainly due to the increase in fat around the organs such as kidneys and mesentery, but no fat was accumulated at the subcutaneous level of the back scapula (Table 3). Perhaps adipose tissue always exists in subcutaneous tissue at a certain level, but it may not be apparent in the CON and OB mice. We could not easily separate subcutaneous adipose tissue by dissection. Of course, we believe that it is unnecessary to use other methods (for example, Soxhlet solvent extraction method) to

extract subcutaneous adipose tissue in the present study. In contrast, in the ground squirrels, fat accumulation was not only increased around the organs including the kidney and mesentery, the subcutaneous fat content of the back scapula also increased significantly after the fattening before hibernation (Table 3). The fattening period before hibernation is a transition period from active to hibernation, in which the ground squirrels prepare for the hibernation period to successfully cope with fasting, disuse, hypoxia and other conditions (Chang et al. 2020). Brown adipose is located in the

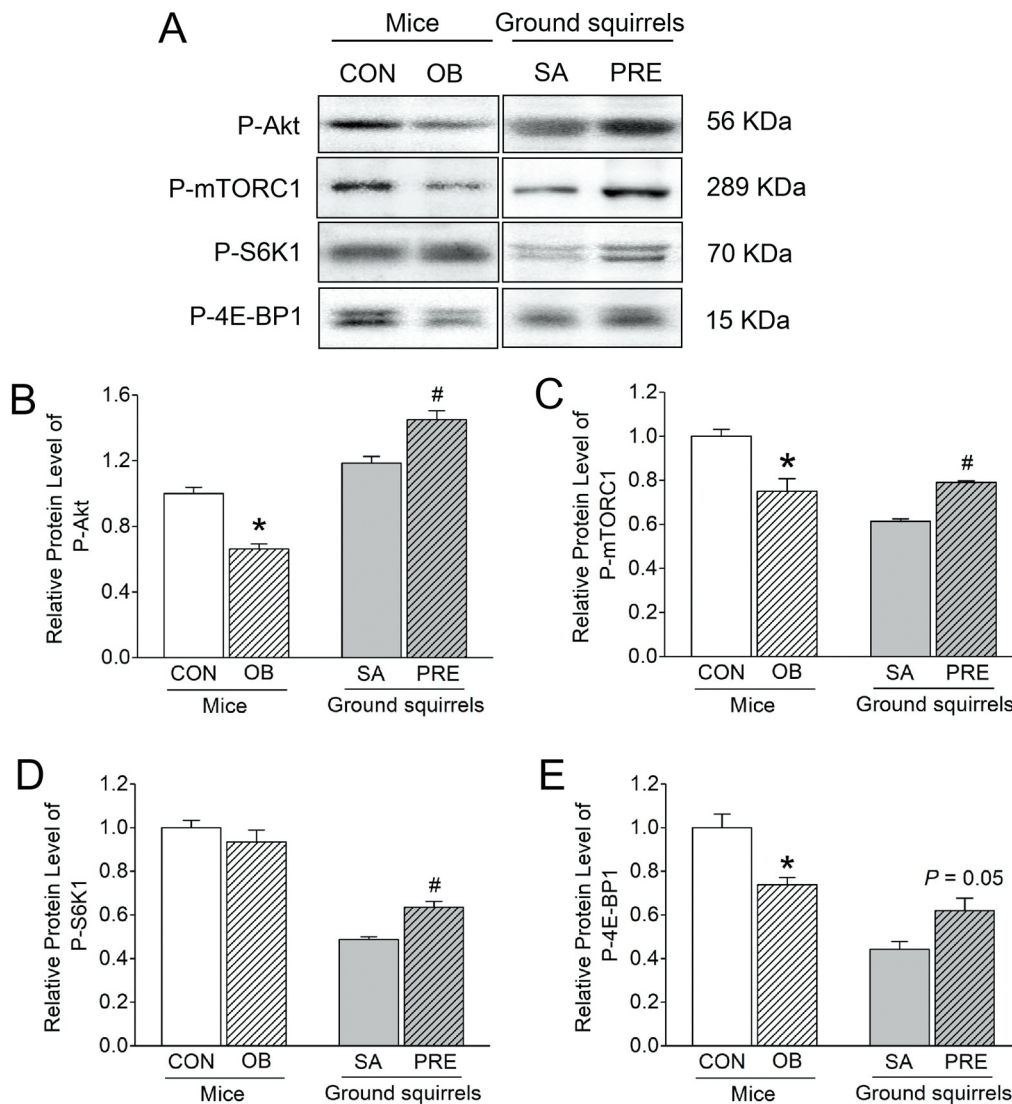


**Fig. 6.** The protein expression levels of P-Akt, P-mTORC1, P-S6K1 and P-4E-BP1. (A) Representative immunoblots of P-Akt, P-mTORC1, P-S6K1 and P-4E-BP1 in gastrocnemius muscles in each group. (B) The relative protein expression level of P-Akt in mice and Daurian ground squirrels. (C) The relative protein expression level of P-mTORC1 in mice and Daurian ground squirrels. (D) The relative protein expression level of P-S6K1 in mice and Daurian ground squirrels. (E) The relative protein expression level of P-4E-BP1 in mice and Daurian ground squirrels. CON: control mice, OB: mice after 3 months of ingesting high fat diet, SA: summer active Daurian ground squirrels, PRE: pre-hibernation, squirrels that finished natural fattening, sacrificed in late-autumn (end of September, 30–40 d before hibernation). Values are mean  $\pm$  SEM,  $n = 6$ . \* $p < 0.05$  compared with CON group. # $p < 0.05$  compared with SA group.

subcutaneous area of the back scapula (Smith and Hock 1963), which is considered to be the main contributor to rapid heat production that quickly restores body temperature and metabolic rate during interbout arousals period (Ballinger and Andrews 2018). Therefore, the location and degree of fat accumulation are different in the pathological obesity and healthy obesity models.

In the present study, the muscle wet weight, the ratio of muscle wet weight/body weight and the CSA of the gastrocnemius muscle were significantly decreased by 8.8%, 17.4% and 14.7%, respectively, in the OB mice compared with the CON group (Figs. 1 and 2). Additionally, the percentage of MHC I fiber (slow-twitch fiber) isoform was significantly increased by 58.1% (Fig. 2), which is consistent with the increase in type I fiber in gastrocnemius and plantaris muscles of male C57BL/6J mice induced by 8-week high-fat diet (Shortreed et al. 2009). Furthermore, the protein expression level of MuRF-1 (one of atrogenes) was significantly increased by 18.1% (Fig. 3B). The above results indicated an atrophy in gastrocnemius muscle of the OB mice. Similarly, the cross-sectional area of gastrocnemius muscle fiber was significantly decreased by 22.9% in the male obese Wistar rats induced by a 16-week high-fat and high-carbohydrate Western-type diet (Sishi et al.

2011). Muscle atrophy also occurred in adult BALB/c mice fed a high-fat diet for 10 weeks and the degree of atrophy was soleus muscle > gastrocnemius muscle > tibialis anterior muscle (Adhikary et al. 2019). Atrophy of the tibialis anterior muscle was also found in male 12-week-old C57BL/10 mice fed on a high-fat diet for 38 weeks (Abrigo et al. 2016). However, there was no change in the muscle weight of gastrocnemius muscle (Fig. 1A), the CSA of muscle fibers, the proportion of MHC I in muscle fibers (Fig. 2), the expression levels of MuRF-1 and atrogen-1 in the PRE ground squirrels (Fig. 3) compared with the SA group, which indicated that the gastrocnemius muscle was maintained in PRE ground squirrels. The significant decrease in the ratio of muscle wet weight/body weight (more severe than OB mice, Fig. 1B) is due to the rapid increase in body weight, which indicates severe obesity. Consistent with our previous research, the plantaris muscle and extensor digitorum longus muscle were also maintained in PRE ground squirrels compared with the SA group (Zhang et al. 2019; Ma et al. 2019). Thus, after the fat accumulation, the gastrocnemius muscle showed atrophy in the OB mice, but was maintained in the PRE ground squirrels.

In the present study, the protein expression

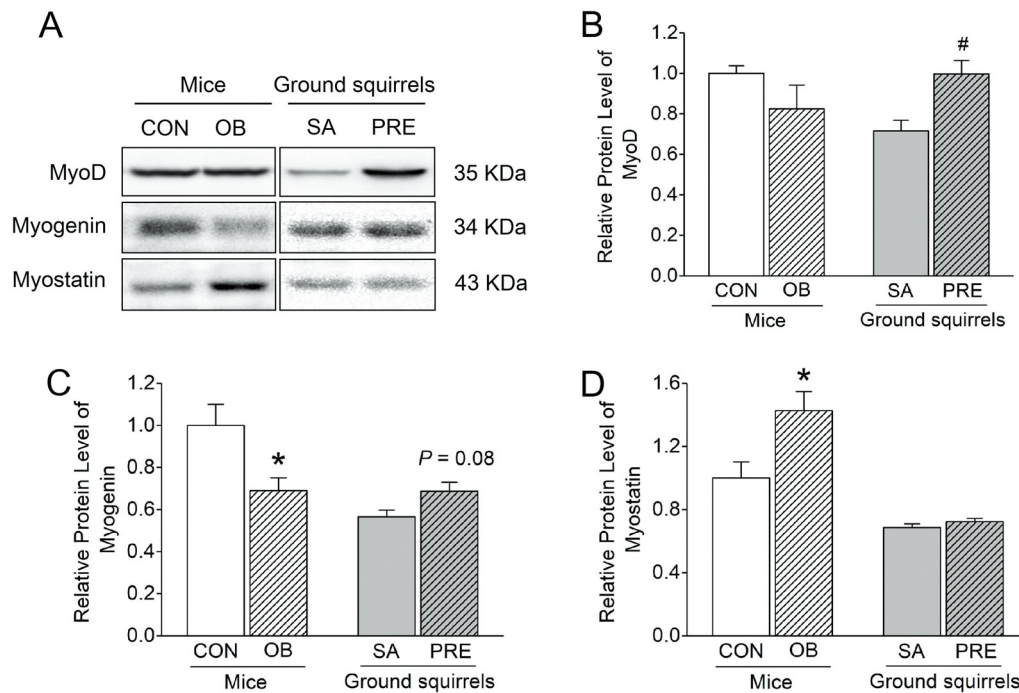


**Fig. 7.** The protein expression levels of MyoD, myogenin and myostatin. (A) Representative immunoblots of MyoD, myogenin and myostatin in gastrocnemius muscles in each group. (B) The relative protein expression level of MyoD in mice and Daurian ground squirrels. (C) The relative protein expression level of myogenin in mice and Daurian ground squirrels. (D) The relative protein expression level of myostatin in mice and Daurian ground squirrels. CON: control mice, OB: mice after 3 months of ingesting high fat diet, SA: summer active Daurian ground squirrels, PRE: pre-hibernation, squirrels that finished natural fattening, sacrificed in late-autumn (end of September, 30–40 d before hibernation). Values are mean  $\pm$  SEM,  $n = 6$ . \* $p < 0.05$  compared with CON group. # $p < 0.05$  compared with SA group.

levels related to protein degradation were different in pathologically obese mice and healthy obese ground squirrels. First, the protein expression levels of calpain1 and calpain2 were significantly increased, while calpastatin (the endogenous inhibitor of calpains) showed no change in the OB mice (Fig. 4). However, in the PRE ground squirrels, the protein expression levels of calpain1, calpain2 and calpastatin showed no change in gastrocnemius muscle compared with the SA group (Fig. 4). Therefore, the differential calpain activation is involved in the mechanisms of muscle atrophy in pathological obesity mice and remarkable ability of muscle maintenance in healthy obese ground squirrels. Our previous research showed that the homeostasis of Ca<sup>2+</sup> concentration plays an important role in the calpain system regulation and anti-atrophy in skeletal muscle of the Daurian ground squirrels during hibernation; meanwhile, the concentration of Ca<sup>2+</sup> in the gastrocnemius muscle rises during hibernation and returns to normal post-hibernation (Fu et al. 2016). Our recent study shows that there is no change in the cytoplasmic Ca<sup>2+</sup> level in the plantaris or adductor magnus muscle in the PRE group compared to the SA ground squirrels (Zhang et al. 2020). Therefore, our study suggests that the homeostasis of cytosolic calcium might be involved in the inactivation of the

calpain system in the gastrocnemius muscle of PRE ground squirrels compared with the SA group. Calpain system has many substrates including cytoskeleton proteins and sarcomeric proteins (Goll et al. 2003), which can reflect the activity of calpain (Dina et al. 2018; Huang and Zhu 2016). Desmin is an intermediate fibrin located around the Z line of skeletal muscles and can be rapidly degraded by calpain (Tokuyasu et al. 1983). We found that the protein expression level of desmin was significantly reduced in the OB mice (Fig. 4), indicating an increase in calpain activity. However, no change was detected in desmin protein expression in the PRE ground squirrels compared with SA group (Fig. 4), which indicated the inactivated calpain. Similarly, troponin T, another substrate of calpain system, which is one of the components of sarcomeric proteins, also significantly decreased in the OB mice, but showed no change in the PRE ground squirrels (Fig. 4). Thus, our study suggests that the calpain system might play an important role in the mechanism of muscle atrophy and anti-atrophy in pathological obesity and healthy obesity models.

The increased calpain activity can lead to an increase in the expression of proteins in the ubiquitin-proteasome pathway (Smith et al. 2008). In the ubiquitin-proteasome pathway, MuRF-1 can bind to

**Table 4.** The relative protein expression levels

	Pathway	Proteins	OB vs. CON	PRE vs. SA
Protein degradation	ubiquitin-proteasome pathway	MuRF-1	18.1% *	8.1%
		atrogen-1	11.3%	-0.9%
	calpain pathway	calpain1	60.1% *	-7.4%
		calpain2	22.4% *	3.1%
		calpastatin	-2.7%	4.1%
		desmin	-33.6% *	7.6%
		troponin T	-29.8% *	6.7%
	autophagy lysosomal pathway	Beclin-1	9.0%	-11.8% #
		LC3-II	7.8%	-35.5% #
	Protein synthesis	PI3K/AKT/mTOR pathway	P-Akt	-33.8% *
P-mTORC1			-25.0% *	28.9% #
P-S6K1			-6.5%	30.5% #
P-4E-BP1			-26.1% *	40.1% ( <i>p</i> = 0.05)
Cell regeneration		MyoD	-17.5%	39.2% #
		myogenin	-31.0% *	21.6% ( <i>p</i> = 0.08)
		myostatin	42.7% *	5.5%

Compared with the CON group, the protein expression level changes in the OB group are shown in the fourth column. Similarly, compared with the SA group, the protein expression level changes in the PRE group are shown in the fifth column. CON: control mice, OB: mice after 3 months of ingesting high fat diet, SA: summer active Daurian ground squirrels, PRE: pre-hibernation, squirrels that finished natural fattening, sacrificed in late-autumn (end of September, 30–40 d before hibernation). Values are mean ± SEM, *n* = 6. \**p* < 0.05 compared with CON group. #*p* < 0.05 compared with SA group.

and induce myosin heavy chain degradation, which contributes to muscle atrophy (Egerman and Glass 2014). Our results showed that the protein expression of MuRF-1 was significantly increased, while atrogen-1 showed no change in the gastrocnemius muscle of the OB mice compared with the CON group (Fig. 3), which suggested that the ubiquitin-proteasome pathway was activated in pathologically obese mice. Similarly, there was a significant increase in the protein expression level of MuRF-1 in the gastrocnemius muscle of male Wistar rats fed a high-fat and high-carbohydrate diet for 16 weeks, while atrogen-1 showed an increased trend but no significant difference ( $p = 0.06$ ) in the obese rats (Sishi et al. 2011). Sulekha et al. also reported that the mRNA level of MuRF-1 was significantly increased in the obese mice fed with a high-fat diet compared with the control group, and that there was no change in the mRNA level of atrogen-1 (Adhikary et al. 2019). Our data suggested that the MuRF-1 was more sensitive than atrogen-1 in the high-fat diet-induced obesity model. Tumor necrosis factor  $\alpha$  (TNF- $\alpha$ ) regulates different

E3s (Sishi et al. 2011). Nuclear factor kappa-B (NF- $\kappa$ B) activated by I $\kappa$ B kinase b (IKKb) specifically acts on the activation of MuRF-1 instead of atrogen-1, while p38 mitogen-activated protein kinase (p38 MAPK) acts on the activation of atrogen-1 (Glass 2005). The expression of TNF- $\alpha$  was significantly increased in the skeletal muscle of obese Male Wistar rats induced by high-fat diet (Borst and Conover 2005). Thus, we assumed that TNF- $\alpha$  and NF- $\kappa$ B signals were involved in obese muscular atrophy induced by the high-fat diet, and the difference in NF- $\kappa$ B and p38 MAPK activity resulted in different sensitivities of MuRF-1 and atrogen-1 in the high-fat diet-induced obesity model. However, there were no changes in the protein expression levels of atrogen-1 and MuRF-1 between the PRE and SA ground squirrels (Fig. 3). In addition, the present study showed that the protein levels of Beclin-1 and LC3-II were unchanged in the gastrocnemius muscle between the OB and CON mice (Fig. 5), which indicated that the autophagy lysosomal pathway was not activated in the OB mice. Similarly, the protein level

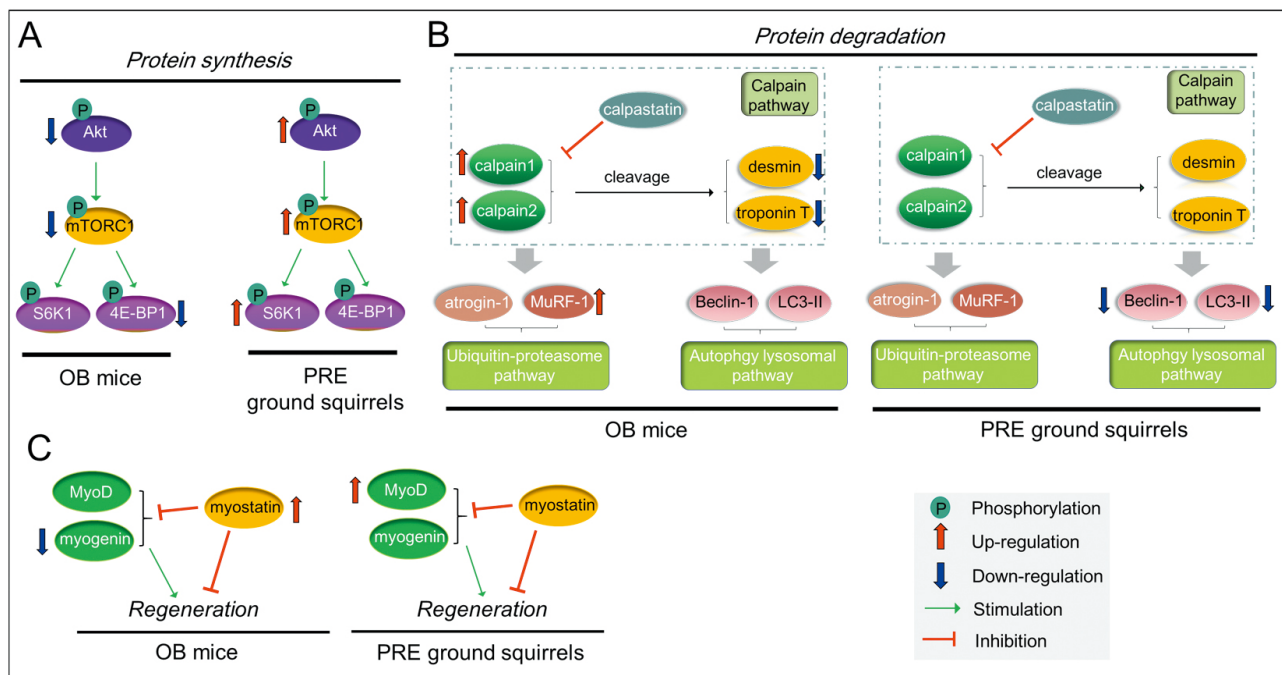


**Fig. 8.** Diagrammatic representation of the protein metabolism and cell regeneration in skeletal muscle of two obesity models. (A) The change in protein synthesis. In the OB mice, the expression levels of P-Akt, P-mTORC1 and P-4E-BP1 decreased significantly. In the PRE ground squirrels, the expression levels of P-Akt, P-mTORC1 and P-S6K1 increased significantly. (B) The change in protein degradation. In the OB mice, the expression levels of calpain1, calpain2 and MuRF-1 increased significantly, and the expression levels of desmin and troponin T decreased significantly. In the PRE ground squirrels, the expression levels of beclin-1 and LC3-II decreased significantly. (C) The change in cell regeneration. In the OB mice, the expression level of myostatin increased significantly, and the expression level of myogenin decreased significantly. In the PRE ground squirrels, the expression level of MyoD increased significantly. OB: mice after 3 months of ingesting high fat diet, PRE: pre-hibernation, squirrels that finished natural fattening, sacrificed in late-autumn (end of September, 30–40 d before hibernation). P-Akt, phosphorylated protein kinase B; P-mTORC1, phosphorylated mammalian target of rapamycin in complex 1; P-S6K1, phosphorylated ribosomal protein S6 kinase 1; P-4E-BP1, phosphorylated 4E binding protein 1; MuRF-1, muscle ring finger-1; LC3, microtubule-associated protein 1A/1B-light chain 3; MyoD, myogenicity differentiation factor.

of LC3 was unchanged in the gastrocnemius muscle of C57BL/6 male mice induced by a 10-week high-fat diet (Herrenbruck and Bollinger 2019). Beclin-1 and LC3-II/I also showed no difference between the obesity and control groups in the soleus muscle and plantaris muscle of female Sprague Dawley rats induced by a 16-week high-fat diet (Campbell et al. 2015). Moreover, the expression of Beclin-1 also showed no change in the soleus and gastrocnemius muscle of obese male C57BL/6 mice fed a high-fat diet for 20 weeks (Zhang et al. 2019). However, the expression of Beclin-1 and LC3-II were significantly decreased in the gastrocnemius muscle in PRE ground squirrels (Fig. 5), which was different from our recent report showing that the expression of Beclin-1 was increased in the soleus muscle of the PRE Daurian ground squirrels compared with the SA group (Chang et al. 2020). We assumed that the autophagy activation is muscle type specific. Thus, the increased levels of proteins in the calpain system and the ubiquitin-proteasome pathway might be involved in the increased protein degradation in the gastrocnemius muscle of pathological obesity induced by a high-fat diet, further contributing to muscle atrophy. However, compared with the SA ground squirrels, the decrease in the level of proteins from the autophagy lysosomal pathway might be involved in the reduced protein degradation in healthy obesity caused by fattening before hibernation, further contributing to preventing muscle atrophy.

The Akt/mTOR pathway plays a critical role in skeletal muscle protein synthesis (Gao et al. 2018). In the present study, the protein levels of P-Akt and P-mTORC1 showed a significant reduction, while their downstream effector, P-4E-BP1, showed a significant decrease and P-S6K1 showed no change in the OB mice compared with the control group (Fig. 6), which is consistent with the findings in the plantaris muscle of male obese C57BL/6 mice induced by a 14-week high-fat and low-carbohydrate diet, the gastrocnemius muscle of male obese Wistar rats induced by a 16-week high-fat and high-carbohydrate Western-type diet, and the gastrocnemius muscle of male obese C57BL/6 mice induced by a 10-week high-fat diet (Sishi et al. 2011; Sitnick et al. 2009; Tong et al. 2019). However, the expression levels of P-Akt, P-mTORC1 and P-S6K1 significantly increased, and the expression level of P-4E-BP1 had no significant difference but showed an increased trend ( $p = 0.05$ ) in PRE ground squirrels compared to those in the SA group (Fig. 6), which might contribute to preventing the gastrocnemius muscle atrophy in healthy obese ground squirrels. Moreover, P-Akt can not only activate mTOR, but also prevent the activation of the atrogen-1 MuRF-1 in the ubiquitin-proteasome pathway and LC3 in the autophagy

lysosomal pathway, which can inhibit the degradation of proteins (Schiaffino and Mammucari 2011; Stitt et al. 2004). In our study, the expression of P-Akt in obese mice was significantly reduced (Fig. 6), which suggests that the inhibitory effect of Akt on protein degradation was weakened. Additionally, the significant increase in P-Akt expression in the PRE ground squirrels also suggests that the inhibition of protein degradation was enhanced (Fig. 6). Taken together, the reduction in the levels of proteins in the Akt/mTOR pathway might involve the decrease in protein synthesis in the gastrocnemius muscle of pathological obesity induced by a high-fat diet, further promoting muscle atrophy. However, compared with the SA ground squirrels, the enhanced Akt/mTOR pathway protein expression levels might be involved in the increased protein synthesis in healthy obesity caused by fattening before hibernation, further contributing to the prevention of muscle atrophy.

Our data showed that the expression level of myogenin proteins in OB mice was significantly reduced, with the increase of myostatin compared with the CON group, however, MyoD showed no change between the OB and the CON mice (Fig. 7). The results indicated that the pathological obesity induced by a high-fat diet caused a decrease in skeletal muscle cell regeneration process. Similar to our study, the mRNA levels of myogenin and MyoD decreased significantly, while myostatin increased significantly in muscles in 8-week old male BALB/c mice fed a high-fat diet for 10 weeks (Adhikary et al. 2019). Moreover, in male wild-type C57/black6j mice fed a high-fat diet for one month, the mRNA level of myostatin was significantly increased in the tibialis anterior muscle (Allen et al. 2008). In contrast, the protein expression level of MyoD was significantly increased and the expression level of myogenin had no significant difference but showed an increased trend ( $p = 0.08$ ), while the myostatin level showed no change in the PRE ground squirrels compared with the SA group (Fig. 7), which suggests that an increase in skeletal muscle regeneration occurs in the healthy obesity induced by fattening before hibernation. Myostatin negatively regulates Akt signaling in skeletal muscle (Sartori et al. 2009; Trendelenburg et al. 2009). Previous studies have reported that myostatin can up-regulate atrogen-1 and MuRF-1 in cultured muscle cells (Bonaldo and Sandri 2013), which indicates that myostatin is a negative regulator of muscle growth. In the current study, both the expression of myostatin and MuRF-1 increased significantly in the pathological obesity model, which indicates that myostatin had a regulatory effect and that myogenesis was reduced. MyoD is a substrate of atrogen-1, so atrogen-1 plays a negative regulatory role in myogenesis (De Larichaudy et al. 2012; Lokireddy et

al. 2012). Desmin is not only a substrate of the calpain system, but also an intermediate filament protein expressed during muscle differentiation. A decrease in desmin is a signal of impaired muscle fiber maturation (Hawke et al. 2003). Our results showed that desmin expression was significantly decreased in the OB mice, but showed no change in the PRE ground squirrels, which suggested that the muscle fiber maturation is impaired in the OB mice, but not in the PRE ground squirrels. Thus, pathological obesity induced by a high-fat diet caused a decline in the expressions of proteins related to cell regeneration, while healthy obesity caused by pre-hibernation fattening showed an increase in protein expressions related to cell regeneration, which might be involved in the mechanism of muscle atrophy and anti-muscle atrophy in obese mice and ground squirrels, respectively.

## CONCLUSIONS

In conclusion, the gastrocnemius muscle showed atrophy in pathological obese mice induced by high-fat diet, but it showed anti-atrophy in healthy obese ground squirrels caused by pre-hibernation fattening. The decrease in the protein expression levels of the Akt/mTOR pathway and cell regeneration, the increase in the protein expression levels of the calpain system and ubiquitin-proteasome pathway were involved in the mechanism of muscle atrophy in the gastrocnemius muscle of the OB mice. However, the increased protein expression levels of the Akt/mTOR pathway and cell regeneration, and the decreased protein expression levels of the autophagy lysosomal pathway, were involved in the mechanism of anti-atrophy in gastrocnemius muscle of the healthy obese ground squirrels fattened before hibernation. The present study not only clarified the differential protein metabolism and regeneration in gastrocnemius muscles in high-fat diet fed mice and pre-hibernation Daurian ground squirrels, but also provided experimental evidence for screening key targets for anti-obesity muscular atrophy in fattening ground squirrels before hibernation.

## List of abbreviations

OB, obesity group.  
 CON, control group.  
 PRE, pre-hibernation.  
 SA, summer active.  
 IGF-1, insulin like grow factor-1.  
 Akt, protein kinase B.  
 mTORC1, mammalian target of rapamycin in complex 1.

S6K1, ribosomal protein S6 kinase 1.  
 4E-BP1, 4E binding protein 1.  
 MuRF-1, muscle ring finger-1.  
 LC3, Microtubule-associated protein 1A/1B-light chain 3.  
 MyoD, myogenicity differentiation factor.  
 CSA, cross-sectional area.  
 TNF- $\alpha$ , Tumor necrosis factor  $\alpha$ .  
 NF- $\kappa$ B, Nuclear factor kappa-B.  
 IKKb, I $\kappa$ B kinase b.  
 p38 MAPK, p38 mitogen-activated protein kinase.

**Acknowledgments:** This study was supported by funds from the National Nature Science Foundation of China (31640072), the Shaanxi Province Natural Science Basic Research Program (2020JM-428). We sincerely thank Yihan Wang and Yutong Wang for helping us revise the English writing.

**Authors' contributions:** Conceived and designed the experiments: HC and YG. Performed the experiments: XY, QN, XG, SS, NH and RF. Analyzed the data: HC, XY, QN and HW. Wrote the paper: QN and HC. All authors read and approved the final manuscript.

**Competing interests:** XY, QN, XG, SS, NH, HW, RF, YG, and HC declare that they have no conflict of interests.

**Availability of data and materials:** The datasets used or analysed during the current study are available from the corresponding author upon reasonable request.

**Consent for publication:** All authors have read and approved the submission of this manuscript to *Zoological Studies*.

**Ethics approval consent to participate:** All animal experiments were approved by the Experimental Animal Protection Committee of the Ministry of Health of the People's Republic of China.

## REFERENCES

- Abrigo J, Rivera JC, Aravena J, Cabrera D, Simon F, Ezquer F et al. 2016. High fat diet-induced skeletal muscle wasting is decreased by mesenchymal stem cells administration: Implications on oxidative stress, ubiquitin proteasome pathway activation, and myonuclear apoptosis. *Oxid Med Cell Longev*. doi:10.1155/2016/9047821.
- Adhikary S, Kothari P, Choudhary D, Tripathi AK, Trivedi R. 2019. Glucocorticoid aggravates bone micro-architecture deterioration and skeletal muscle atrophy in mice fed on high-fat diet. *Steroids* 149:108416. doi:10.1016/j.steroids.2019.05.008.



- Akhmedov D, Berdeaux R. 2013. The effects of obesity on skeletal muscle regeneration. *Front Physiol* **4**:371. doi:10.3389/fphys.2013.00371.
- Allen DL, Cleary AS, Speaker KJ, Lindsay SF, Uyenishi J, Reed JM et al. 2008. Myostatin, activin receptor iib, and follistatin-like-3 gene expression are altered in adipose tissue and skeletal muscle of obese mice. *Am J Physiol-Endoc M* **294**:E918–E927. doi:10.1152/ajpendo.00798.2007.
- Andres-Mateos E, Brinkmeier H, Burks TN, Mejias R, Files DC, Steinberger M et al. 2013. Activation of serum/glucocorticoid-induced kinase 1 (SGK1) is important to maintain skeletal muscle homeostasis and prevent atrophy. *EMBO Mol Med* **5**:80–91. doi:10.1002/emmm.201201443.
- Ballinger MA, Andrews MT. 2018. Nature's fat-burning machine: Brown adipose tissue in a hibernating mammal. *J Exp Biol* **221**(Pt Suppl 1):jeb162586. doi:10.1242/jeb.162586.
- Bodine SC, Baehr LM. 2014. Skeletal muscle atrophy and the E3 ubiquitin ligases MuRF1 and MAFbx/atrogen-1. *Am J Physiol-Endoc M* **307**:E469–E484. doi:10.1152/ajpendo.00204.2014.
- Bodine SC, Latres E, Baumhueter S, Lai VKM, Nunez L, Clarke BA et al. 2001. Identification of ubiquitin ligases required for skeletal muscle atrophy. *Science* **294**:1704–1708. doi:10.1126/science.1065874.
- Bonaldo P, Sandri M. 2013. Cellular and molecular mechanisms of muscle atrophy. *Dis Model Mech* **6**:25–39. doi:10.1242/dmm.010389.
- Borst SE, Conover CF. 2005. High-fat diet induces increased tissue expression of TNF- $\alpha$ . *Life Sci* **77**:2156–2165. doi:10.1016/j.lfs.2005.03.021.
- Campbell TL, Mitchell AS, McMillan EM, Bloemberg D, Pavlov D, Messa I et al. 2015. High-fat feeding does not induce an autophagic or apoptotic phenotype in female rat skeletal muscle. *Exp Biol Med* (Maywood) **240**:657–668. doi:10.1177/1535370214557223.
- Chang H, Jiang S-F, Dang K, Wang H-P, Xu S-H, Gao Y-F. 2016. iTRAQ-based proteomic analysis of myofibrillar contents and relevant synthesis and proteolytic proteins in soleus muscle of hibernating Daurian ground squirrels (*Spermophilus dauricus*). *Proteome Sci* **14**:16. doi:10.1186/s12953-016-0105-x.
- Chang H, Lei T, Ma X, Zhang J, Wang H, Zhang X et al. 2018. Muscle-specific activation of calpain system in hindlimb unloading rats and hibernating daurian ground squirrels: A comparison between artificial and natural disuse. *J Comp Physiol B* **188**:863–876. doi:10.1007/s00360-018-1176-z.
- Chang H, Peng X, Yan X, Zhang J, Xu S, Wang H et al. 2020. Autophagy and Akt-mTOR signaling display periodic oscillations during torpor-arousal cycles in oxidative skeletal muscle of Daurian ground squirrels (*Spermophilus dauricus*). *J Comp Physiol B* **190**:113–123. doi:10.1007/s00360-019-01245-5.
- Chen B, Shan T. 2019. The role of satellite and other functional cell types in muscle repair and regeneration. *J Muscle Res Cell M* **40**:1–8. doi:10.1007/s10974-019-09511-3.
- De Larichaudy J, Zufferli A, Serra F, Isidori AM, Naro F, Dessalle K et al. 2012. Tnf- $\alpha$ - and tumor-induced skeletal muscle atrophy involves sphingolipid metabolism. *Skelet Muscle* **2**:2. doi:10.1186/2044-5040-2-2.
- D'Souza DM, Trajcevski KE, Al-Sajee D, Wang DC, Thomas M, Anderson JE et al. 2015. Diet-induced obesity impairs muscle satellite cell activation and muscle repair through alterations in hepatocyte growth factor signaling. *Physiol Rep* **3**:e12506. doi:10.14814/phy2.12506.
- Dina A, Inga R, Alexandra V, Eitan S, Shenhav C. 2018. Gsk3- $\beta$  promotes calpain-1-mediated desmin filament depolymerization and myofibril loss in atrophy. *J cell biol* **217**:3698–3714. doi:10.1083/jcb.201802018.
- Dumitru A, Radu BM, Radu M, Cretoiu SM. 2018. Muscle changes during atrophy. *In: J. Xiao* (ed.) *Muscle atrophy*, Adv Exp Med Biol No. 1088. pp. 73–92. doi:10.1007/978-981-13-1435-3\_4.
- Egerman MA, Glass DJ. 2014. Signaling pathways controlling skeletal muscle mass. *Crit Rev Biochem Mol* **49**:59–68. doi:10.3109/10409238.2013.857291.
- Fu WW, Hu HX, Dang K, Chang H, Du B, Wu X et al. 2016. Remarkable preservation of Ca<sup>2+</sup> homeostasis and inhibition of apoptosis contribute to anti-muscle atrophy effect in hibernating daurian ground squirrels. *Sci Rep-UK* **6**:27020. doi:10.1038/srep27020.
- Gao Y, Arfat Y, Wang H, Goswami N. 2018. Muscle atrophy induced by mechanical unloading: Mechanisms and potential countermeasures. *Front Physiol* **9**:235. doi:10.3389/fphys.2018.00235.
- Glass DJ. 2005. Skeletal muscle hypertrophy and atrophy signaling pathways. *Int J Biochem Cell B* **37**:1974–1984. doi:10.1016/j.biocel.2005.04.018.
- Goll DE, Thompson VF, Li H, Wei W, Cong J. 2003. The calpain system. *Physiol Rev* **83**:731–801. doi:10.1152/physrev.00029.2002.
- Hawke TJ, Meeson AP, Jiang N, Graham S, Hutcheson K, DiMaio JM et al. 2003. P21 is essential for normal myogenic progenitor cell function in regenerating skeletal muscle. *Am J Physiol-Cell Ph* **285**:C1019–C1027. doi:10.1152/ajpcell.00055.2003.
- Herrenbruck AR, Bollinger LM. 2019. Role of skeletal muscle autophagy in high-fat-diet-induced obesity and exercise. *Nutr Rev* **78**:56–64. doi:10.1093/nutrit/nuz044.
- Hershko A, Ciechanover A. 1998. The ubiquitin system. *Annu rev biochem* **67**:425–479. doi:10.1146/annurev.biochem.67.1.425.
- Hittel DS, Berggren JR, Shearer J, Boyle K, Houmard JA. 2009. Increased secretion and expression of myostatin in skeletal muscle from extremely obese women. *Diabetes* **58**:30–38. doi:10.2337/db08-0943.
- Hsieh YY, Chang CC, Hsu KH, Tsai FJ, Chen CP, Tsai HD. 2008. Effect of exercise training on calpain systems in lean and obese Zucker rats. *Int J Biol Sci* **4**:300–308. doi:10.7150/ijbs.4.300.
- Huang JR, Zhu XP. 2016. The molecular mechanisms of calpains action on skeletal muscle atrophy. *Physiol Res* **65**:547–560. doi:10.33549/physiolres.933087.
- Jackman RW, Kandarian SC. 2004. The molecular basis of skeletal muscle atrophy. *Am J Physiol-Cell Ph* **287**:C834–C843. doi:10.1152/ajpcell.00579.2003.
- Kamine A, Shimozuru M, Shibata H, Tsubota T. 2012. Changes in blood glucose and insulin responses to intravenous glucose tolerance tests and blood biochemical values in adult female Japanese black bears (*Ursus thibetanus japonicus*). *Jpn J Vet Res* **60**:5–13. doi:10.14943/jjvr.60.1.5.
- Klionsky DJ, Abdalla FC, Abeliovich H, Abraham RT, Acevedo-Arozena A, Adeli K et al. 2012. Guidelines for the use and interpretation of assays for monitoring autophagy. *Autophagy* **8**:445–544. doi:10.4161/auto.19496.
- Lee S, Kim M-B, Kim C, Hwang J-K. 2018. Whole grain cereal attenuates obesity-induced muscle atrophy by activating the PI3K/Akt pathway in obese C57BL/6N mice. *Food Sci Biotechnol* **27**:159–168. doi:10.1007/s10068-017-0277-x.
- Lee SJ. 2004. Regulation of muscle mass by myostatin. *Annu Rev Cell Dev Biol* **20**:61–86. doi:10.1146/annurev.cellbio.20.012103.135836.
- Li Z, Ji GE. 2018. Ginseng and obesity. *J Ginseng Res* **42**:1–8. doi:10.1016/j.jgr.2016.12.005.
- Lokireddy S, Wijesoma IW, Sze SK, McFarlane C, Kambadur

- R, Sharma M. 2012. Identification of atrogin-1-targeted proteins during the myostatin-induced skeletal muscle wasting. *Am J Physiol-Cell Ph* **303**:C512–C529. doi:10.1152/ajpcell.00402.2011.
- Ma X, Chang H, Wang Z, Xu S, Peng X, Zhang J et al. 2019. Differential activation of the calpain system involved in individualized adaptation of different fast-twitch muscles in hibernating daurian ground squirrels. *J Appl Physiol (Bethesda, Md. : 1985)* **127**:328–341. doi:10.6084/m9.figshare.8061893.
- Mei Y, Ramanathan A, Glover K, Stanley C, Sanishvili R, Chakravarthy S et al. 2016. Conformational flexibility enables the function of a BECN1 region essential for starvation-mediated autophagy. *Biochemistry* **55**:1945–1958. doi:10.1021/acs.biochem.5b01264.
- Mizushima N, Yamamoto A, Matsui M, Yoshimori T, Ohsumi Y. 2004. *In vivo* analysis of autophagy in response to nutrient starvation using transgenic mice expressing a fluorescent autophagosome marker. *Mol Biol Cell* **15**:1101–1111. doi:10.1091/mbc.e03-09-0704.
- Mordier S, Deval C, Bechet D, Tassa A, Ferrara M. 2000. Leucine limitation induces autophagy and activation of lysosome-dependent proteolysis in C2C12 myotubes through a mammalian target of rapamycin-independent signaling pathway. *J Biol Chem* **275**:29900–29906. doi:10.1074/jbc.M003633200.
- Ohno Y, Matsuba Y, Hashimoto N, Sugiura T, Ohira Y, Yoshioka T et al. 2016. Suppression of myostatin stimulates regenerative potential of injured antigravitational soleus muscle in mice under unloading condition. *Int J Med Sci* **13**:680–685. doi:10.7150/ijms.16267.
- Rigano KS, Gehring JL, Evans Hutzenbiler BD, Chen AV, Nelson OL, Vella CA et al. 2017. Life in the fat lane: Seasonal regulation of insulin sensitivity, food intake, and adipose biology in brown bears. *J Comp Physiol B* **187**:649–676. doi:10.1007/s00360-016-1050-9.
- Sala D, Ivanova S, Plana N, Ribas V, Duran J, Bach D et al. 2014. Autophagy-regulating TP53INP2 mediates muscle wasting and is repressed in diabetes. *J Clin Invest* **124**:1914–1927. doi:10.1172/JCI72327.
- Sandri M. 2008. Signaling in muscle atrophy and hypertrophy. *Physiology* **23**:160–170. doi:10.1152/physiol.00041.2007.
- Sartorelli V, Fulco M. 2004. Molecular and cellular determinants of skeletal muscle atrophy and hypertrophy. *Sci STKE* **2004**:re11. doi:10.1126/stke.2442004re11.
- Sartori R, Milan G, Patron M, Mammucari C, Blaauw B, Abraham R et al. 2009. Smad2 and 3 transcription factors control muscle mass in adulthood. *Am J Physiol Cell Physiol* **296**:C1248–1257. doi:10.1152/ajpcell.00104.2009.
- Schiaffino S, Dyar KA, Ciciliot S, Blaauw B, Sandri M. 2013. Mechanisms regulating skeletal muscle growth and atrophy. *Febs J* **280**:4294–4314. doi:10.1111/febs.12253.
- Schiaffino S, Mammucari C. 2011. Regulation of skeletal muscle growth by the IGF1-Akt/PKB pathway: Insights from genetic models. *Skelet Muscle* **1**:4. doi:10.1186/2044-5040-1-4.
- Shortreed KE, Krause MP, Huang JH, Dhanani D, Moradi J, Ceddia RB et al. 2009. Muscle-specific adaptations, impaired oxidative capacity and maintenance of contractile function characterize diet-induced obese mouse skeletal muscle. *PLoS ONE* **4**:e7293. doi:10.1371/journal.pone.0007293.
- Sishi B, Loos B, Ellis B, Smith W, du Toit EF, Engelbrecht A-M. 2011. Diet-induced obesity alters signalling pathways and induces atrophy and apoptosis in skeletal muscle in a prediabetic rat model. *Exp Physiol* **96**:179–193. doi:10.1113/expphysiol.2010.054189.
- Sitnick M, Bodine SC, Rutledge JC. 2009. Chronic high fat feeding attenuates load-induced hypertrophy in mice. *J Physiol-London* **587**:5753–5765. doi:10.1113/jphysiol.2009.180174.
- Smith IJ, Lecker SH, Hasselgren PO. 2008. Calpain activity and muscle wasting in sepsis. *Am J Physiol-Endoc M* **295**:E762–E771. doi:10.1152/ajpendo.90226.2008.
- Smith RE, Hock RJ. 1963. Brown fat: Thermogenic effector of arousal in hibernators. *Science* **140**:199–200. doi:10.1126/science.140.3563.199.
- Stitt TN, Drujan D, Clarke BA, Panaro F, Timofeyeva Y, Kline WO et al. 2004. The IGF-1/PI3K/Akt pathway prevents short article expression of muscle atrophy-induced ubiquitin ligases by inhibiting FOXO transcription factors. *Mol Cell* **14**:395–403. doi:10.1016/S1097-2765(04)00211-4.
- Tokuyasu KT, Dutton AH, Singer SJ. 1983. Immunoelectron microscopic studies of desmin (skeleton) localization and intermediate filament organization in chicken skeletal muscle. *J Cell Biol* **96**:1727–1735. doi:10.1083/jcb.96.6.1727.
- Tong T, Kim M, Park T. 2019.  $\alpha$ -Ionone attenuates high-fat diet-induced skeletal muscle wasting in mice *via* activation of camp signaling. *Food Funct* **10**:1167–1178. doi:10.1039/c8fo01992d.
- Trendelenburg AU, Meyer A, Rohner D, Boyle J, Hatakeyama S, Glass DJ. 2009. Myostatin reduces Akt/TORC1/p70S6K signaling, inhibiting myoblast differentiation and myotube size. *Am J Physiol Cell Physiol* **296**:C1258–1270. doi:10.1152/ajpcell.00105.2009.
- Xing X, Sun M-Y, Peng X, Song S-Y, Yang M. 2012. Expression of orexigenic and anorexigenic neuropeptides before and during hibernation in the daurian ground squirrel (*Spermophilus dauricus*). In: T. Ruf, C. Bieber, W. Arnold and E. Millesi (eds.) *Living in a seasonal world: Thermoregulatory and metabolic adaptations*. p 543–556. Springer Berlin Heidelberg, Berlin, Heidelberg. doi:10.1007/978-3-642-28678-0\_47.
- Yang C-X, He Y, Gao Y-F, Wang H-P, Goswami N. 2014. Changes in calpains and calpastatin in the soleus muscle of Daurian ground squirrels during hibernation. *Comp Biochem Phys A* **176**:26–31. doi:10.1016/j.cbpa.2014.05.022.
- Zhang D, Lee JH, Kwak SE, Shin HE, Zhang Y, Moon HY et al. 2019. Effect of a single bout of exercise on autophagy regulation in skeletal muscle of high-fat high-sucrose diet-fed mice. *J Obes Metab Syndr* **28**:175–185. doi:10.7570/jomes.2019.28.3.175.
- Zhang J, Li X, Ismail F, Xu S, Wang Z, Peng X et al. 2020. Priority strategy of intracellular  $Ca^{2+}$  homeostasis in skeletal muscle fibers during the multiple stresses of hibernation. *Cells* **9**:42. doi:10.3390/cells9010042.
- Zhang J, Wei Y, Qu T, Wang Z, Xu S, Peng X et al. 2019. Prosurvival roles mediated by the perk signaling pathway effectively prevent excessive endoplasmic reticulum stress-induced skeletal muscle loss during high-stress conditions of hibernation. *J Cell Physiol* **234**:19728–19739. doi:10.1002/jcp.28572.